VGOS Source Selection Criteria

Bill Petrachenko[1], Patrick Charlot[2], Arnaud Collioud[2], Anthony Searle[1]

Abstract Source structure has long been recognized as a significant risk factor for the broadband method. The issue of greatest concern is that structure related phases and delays will lead to cycle slips during broadband phase connection. These errors are subtle to detect and difficult or impossible to correct after the fact. As the advent of VGOS operations draws near, criteria will be needed to generate lists of candidate VGOS sources that are at the same time strong enough to be detected and simple enough not to cause broadband phase connection errors. The purpose of this study is to propose useful VGOS source selection criteria and to understand their relation to broadband frequency sequences, source lists, and geodetic/astrometric performance. In order to increase the number of available sources, an attempt will be made to find frequency sequences that operate reliably below the typical VGOS flux cut-off of 250 mJy. Candidate source lists will be generated using the Bordeaux VLBI Image Data Base (BVID) as input.

Keywords VGOS, source, selection, criteria

1 Introduction

Source structure is a significant cause of systematic error in geodetic VLBI. It varies with both time and frequency, manifesting in some cases as apparent motion of the source but always as a systematic variation of delay, phase, and amplitude as the length and orientation of the interferometer baseline changes. For VGOS, variation of structure with frequency introduces an additional challenge: it has the potential to compromise phase connection between bands.

Traditionally two approaches have been considered for mitigating the negative impact of source structure. The more active of the two is the application of structure corrections. This involves the use of a high quality source image to calculate delay, phase, and amplitude corrections in the uv-plane (a plane perpendicular to the direction to the source that contains instantaneous projected baseline vectors expressed in units of wavelengths). If corrections have been applied successfully, the source appears as a point source situated at the reference location of the image. Unfortunately, the use of phase closure in VLBI removes all absolute position information from the image, making it difficult to overlay images from one epoch to another and from one frequency band to another, which is a significant challenge for the structure corrections approach. Up to the present time, structure corrections have not produced significant enough performance improvements to be considered for operational use.

The second approach is to generate lists of sources that have acceptably small amounts of structure and to use only those sources. This is the approach taken traditionally and is the approach taken in this paper. Operationally this requires meaningful criteria for selecting sources along with frequent observations of candidate sources to evaluate their changing structure and flux. To be useful, the criteria need to incorporate: correlated flux and structure delay over the uv-plane; the fact that, in broadband delay, dispersive and non-dispersive delays are calculated simultaneously, and the impact of broadband frequency sequences.

If this approach is taken, it is pertinent to ask whether the selection criteria will provide a large

1. Natural Resources Canada
2. Laboratoire d'Astrophysique de Bordeaux

enough sample of sources for VGOS observing. There is some evidence from Monte Carlo simulations [1] that weak improvement in geodetic/astrometric performance results if the number of scheduled sources increases from 32 to 64 with diminishing benefit above 64. However, there are other benefits of increasing the size of the source list, e.g., reduced impact of source structure related systematics, better connection to the ICRF, and improved maintenance of the ICRF. It is difficult to be quantitative about the number of sources required, but it is reasonable that the target should be a list of at least a couple hundred sources. Furthermore, it will be difficult to estimate the number of broadband sources available given that, although plentiful structure data is available at S- and X-bands, little is available at the frequencies planned for the broadband method. For this reason, a criterion for selecting broadband sources based on S/X observations will be useful.

Questions to be answered in this paper include:

- Are there good criteria for evaluating the suitability of broadband sources?
- Will there be at least about two hundred suitable sources for VGOS observing?
- Is it useful to optimize broadband frequency sequences to increase the number of suitable sources?

2 Background

2.1 Bordeaux VLBI Image Database (BVID)

The BVID [2] is used extensively in this study both as a source of S/X-band structural information and as a model for the type of quality metrics that might be used as VGOS broadband source selection criteria. The BVID includes in excess of 1,200 sources, each of which has been observed in both S- and X-band. Although a large number of the BVID sources were observed only once, many were observed in excess of 20 or 30 times. Each time a BVID source is observed, S- and X-band images are produced, and these are then used to calculate a uv-plane distribution of structure delay and visibility. The S- and X-band structure delays are further scaled to reflect the impact of that band on the ionosphere corrected delay. The median structure delay over the uv-plane (scaled according to its impact on the ionosphere corrected delay) forms the basis for the S- and X-band structure indices [see Table 1], and the median visibility is used as a measure of the source compactness. Finally, the total flux is provided, which, when combined with the source visibility, produces the correlated flux over the uv-plane.

Table 1 Structure Index definition [5].

Structure Index (SI)	Median structure delay (ps)
1	0-3
2	3-10
3	10-30
4	>30

2.2 Frequency Sequences

The VGOS broadband system uses four bands in the 3–14 GHz range. Each band has nominally 1 GHz bandwidth with a cumulative data rate for all four bands of 16 Gbps. The exact frequency placement of the bands influences the ability to connect phase between bands. For example, phase connection is improved if: the frequency range from lowest to highest band is decreased; the bands are spread in some optimal fashion instead of, for example, being arranged in groups, or the bandwidth of each band is increased. [Note that although the ability to connect phase improves for narrower sequences, the ability to resolve delay degrades in proportion.] Four sample optimized sequences have been generated, and the fluxes below which the delay resolution peak starts to be mis-identified (assuming integrations of 10 s, SEFDs of 2500 Jy, and the use of 200,000 tries at peak identification) have been determined. The sequences are summarized in Table 2. Note that in all cases, the minimum fluxes are significantly below the typical VGOS flux cut-off of 250 mJ.

Table 2 Frequency Sequence summary.

Seq	BW (MHz)	Data rate (Gbps)	Start (GHz)	Stop (GHz)	Min Flux (mJy)
1	512	15	3.0	9.8	145
2	1024	16	3.0	13.7	120
3	1024	16	3.0	10.8	100
4	1024	32	3.0	10.8	75

2.3 Broadband Delay Calculation

The output of a VLBI correlator is a set of complex correlation coefficients, one for each frequency channel, i.e.,

$$\Gamma_i = A_i e^{-j\phi_i} \tag{1}$$

where A_i is the amplitude of the i^{th} channel and ϕ_i is the phase of the i^{th} channel. The phase can further be expanded as,

$$\phi_i = 2\pi f_i \left(\tau + \frac{K}{{f_i}^2}\right) \tag{2}$$

where f_i is the frequency of the i^{th} channel, τ is the non-dispersive delay of the signal (due to, for example, the interferometer geometry, the neutral atmosphere, the instrumentation, and the offset of the reference oscillators), $\frac{K}{{f_i}^2}$ is the dispersive (phase) delay due to the ionosphere, and K is a factor proportional to the total electron content (TEC) along the line of sight to the source.

Because the ionosphere delay varies with frequency, it can be eliminated if data are taken at more than one band. For legacy S/X systems, a linear delay is calculated separately for both S- and X-band, and then the delays from each of the two bands are combined to produce an ionosphere corrected delay. For VGOS broadband systems, the non-dispersive and dispersive delays are calculated in a single step. A grid of trial values, $\hat{\tau}_m$ and $\hat{K}_n$, are subtracted from τ and K in Equation (2) to give,

$$\Delta\phi_{imn} = 2\pi f_i \left((\tau - \hat{\tau}_m) + \frac{(K - \hat{K}_n)}{{f_i}^2}\right) \tag{3}$$

Then, for each value of m and n, the trial correlation coefficients (i.e. the correlation coefficients with $\hat{\tau}_m$ and $\hat{K}_n$ subtracted, see Equation (3)) are summed over all frequencies to produce the delay resolution function (DRF), i.e.,

$$DRF_{mn} = \sum_i A_i e^{-j\Delta\phi_{imn}} \tag{4}$$

The values of $\hat{\tau}_m$ and $\hat{K}_n$ that maximize DRF_{mn} are the maximum likelihood estimates of τ and K. The DRF for a typical broadband sequence is depicted in Figure 1. The elongated diagonal peak is an indication that the non-dispersive delay and TEC are significantly correlated.

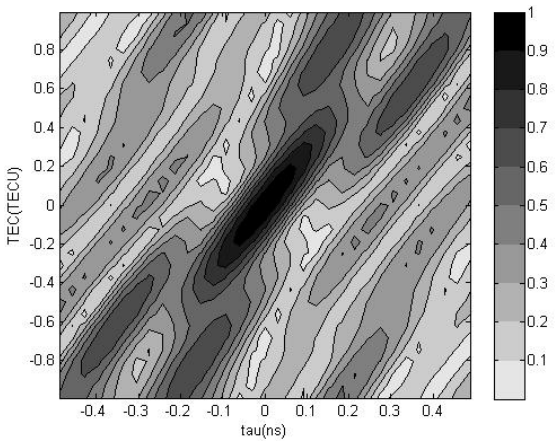

Fig. 1 The delay resolutions function (DRF) for a typical broadband frequency sequence.

3 Broadband Source Selection Criteria

A similar approach to that based on the BVID structure index and source compactness for legacy S/X sources (see Section 2.1) could be extended to broadband delay except that four bands would need to be handled instead of two. Although this provides valuable information about the individual bands, the cumulative effect on the final broadband result is more difficult to assess. Hence it may be efficient and meaningful to find quality factors that consider the whole broadband frequency sequence at the same time. This will be particularly useful when several hundred sources need to be evaluated automatically on a frequent basis.

The broadband DRF suggests a method for doing this. The following steps could be applied to generate uv plots of broadband correlated flux and broadband structure delay bias:

1. Generate high quality source images for each band and align the images relative to each other. [Note: the loss of absolute position information resulting from the use of phase closure makes it impossible to rigorously align the images; hence assumptions are required.]

2. Transform the images to the uv-plane to give correlated fluxes and structure phases at all points in the uv-plane and for the observing frequencies of all broadband channels.
3. For each point in the uv-plane, use the correlated fluxes and structure phases (for each channel) to simulate complex correlation coefficients and input these into the DRF calculation (see Section 2.3).
4. Determine the broadband correlated flux as the height of the DRF peak.
5. Determine the broadband delay bias as the location of the DRF peak.
6. Repeat Steps 3 to 5 for each point in the uv-plane to produce uv plots of broadband correlated flux and broadband structure delay (see Figure 2).

[Note: These plots no longer apply to individual bands (as was the case for the BVID S/X plots) but to the full broadband sequence.]

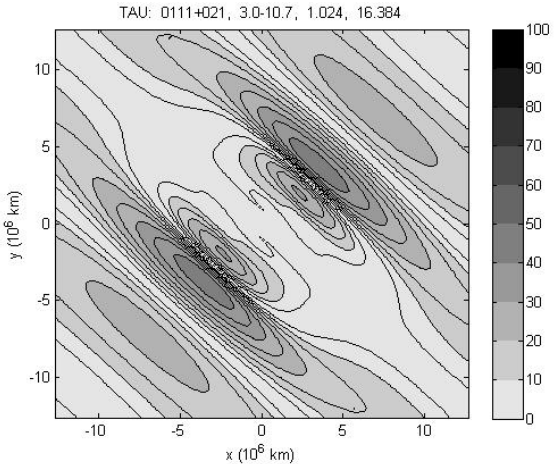

Fig. 2 uv-plot of broadband structure delay for source 0111+021. Source 0111+021 was observed 12 times between 1997 and 2010 and consistently had a structure index of 3 at X-band and a structure index of either 1 or 2 at S-band. Grey scale in the plot is in ps.

This can be taken one step further to consider the impact of correlated flux and source structure on broadband delay precision. The process for doing this involves the addition of gaussian pseudo random noise (prn) values to the source-based correlation coefficients that are input to the DRF calculation. In order to generate realistic noise signals, it is necessary to assume values for integration time, data rate, and antenna SEFD. If the process is repeated a number of times (e.g., 25–50 times) using different prn sequences then the scatter of delay estimates will reflect the expected delay precision. This can be repeated for all points of the uv-plane to produce a uv-plot of expected delay precision (see Figure 3). [Note: These uv-plots depend on assumed values of integration time, data rate, and antenna SEFD and hence are not unique. They need to be scaled if different values of these parameters are appropriate.]

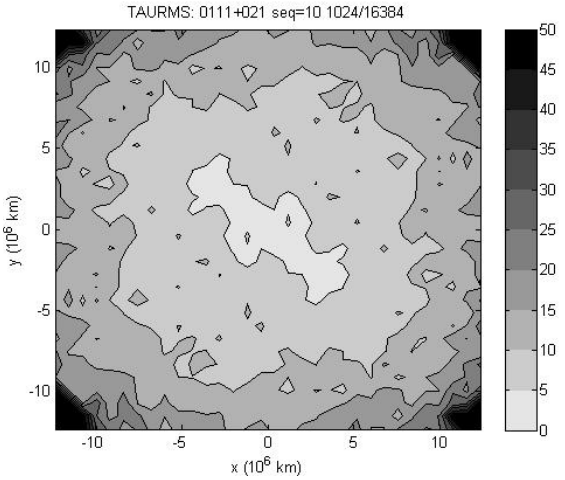

Fig. 3 uv-plot of broadband rms delay error for source 0111+021. Grey scale in the plot is in ps.

4 Number of Broadband Sources

The final goal of the paper is to predict the number of sources that will be available for use with the broadband system. Unfortunately, the current lack of source related data at all frequencies expected for broadband oberving makes this difficult. So the challenge is to find a way to use legacy S/X-band data, which is plentiful, to predict which sources will work with the VGOS broadband systems. Because actual broadband data is not yet available, this cannot be done with a high degree of reliability; however, the conclusions arrived at through the use of S/X-band data should be at least reliable enough to get a rough idea of the number of sources that will be available for use with broadband observing.

A method for doing this was suggested by Arthur Niell in 2006 [3]. It relies on a paper by Fey and Charlot [5] in which S- and X-band elliptical component models were reported for 225 sources. In order to interpolate to arbitrary frequencies, hand picked assumptions were made regarding the spectral indices of the component fluxes. Because each source required individual attention, the approach was applied to only five of the 225 sources [4], making it difficult to draw general conclusions.

In this paper, a single set of spectral rules was applied to each source, making it possible to automate the interpolation process. The rules were: a) hold the S-band component fluxes fixed below 2.3 GHz, falling linearly above 2.3 GHz to zero at 8.5 GHz and b) hold the X-band component fluxes fixed above 8.5 GHz, falling linearly below 8.5 GHz to zero at 2.3 GHz. The only exception was for the main component flux, in which case an exponential was fitted to the S- and X-band values. Based on these rules, component models could be derived at arbitrary frequencies hence simulating actual broadband data.

Through cut and try methods an equation was then developed that combined ratios between S- and X-band median correlated flux, visibility, and structure delay and respective threshold values of the same parameters. The threshold values were then adjusted until the equation had the highest success rate (based on the 225 sources with broadband data simulated from component models) for predicting the truth of specified broadband conditions. The conditions tested are listed in the first column of Table 3 where here the focus was on rms delay error but could be expanded to also include delay bias. The process was repeated for each of the four test frequency sequences proposed in Section 2.2. When tested against the 225 sources with component models, the process was 85% to 90% successful in predicting broadband conditions based on S/X-band data. This was then applied to the full set of sources in the BVID, and the results are summarized in Table 3.

Table 3 Prediction of the number of BVID sources available for broadband observing based on S/X-band correlated flux and struture delay data.

Criterion	Seq#1	Seq#2	Seq#3	Seq#4
90% of uv-plane below 8 ps rms	191	212	213	269
90% of uv-plane below 16 ps rms	269	261	310	388
60% of uv-plane below 8 ps rms	350	408	412	566
60% of uv-plane below 16 ps rms	566	530	644	729

5 Summary and Conclusions

- Frequency sequences were proposed that work significantly below the typical VGOS flux cut-off of 250 mJ.
- A method was proposed for calculating broadband structure delay.
- A method was proposed for predicting expected rms delay error based on both correlated flux and structure phase.
- A method was proposed for using S/X median structure delay, visibility and flux to predict the number of sources available for broadband observing. Based on this method, it is expected that there will be at least 200 sources available for broadband observing.
- It was found that optimized frequency sequences can increase the number of available sources by roughly 50%.

Acknowledgements

This research has made use of material from the Bordeaux VLBI Image Database (BVID): http://www.obs.u-bordeaux1.fr/BVID.

References

1. Searle, A. and Petrachenko, B., “Operational VGOS Scheduling”, 2016, Proceedings of the 9^{th} IVS General Meeting (this volume).
2. Collioud, A. and Charlot, P., “The Bordeaux VLBI Image Data base”, 19th EVGA Working Meeting Proceedings, eds. G. Bourda, P. Charlot, and A. Collioud, 2009.
3. Niell, A., “Source Structure Simulation”, 2006, IVS memo 2006-017v01, ftp://ivscc.gsfc.nasa.gov/pub/memos/ivs-2006-017v01.pdf
4. Niell, A., “Source Structure Examples”, 2006, IVS memo 2006-018v01, ftp://ivscc.gsfc.nasa.gov/pub/memos/ivs-2006-018v01.pdf
5. Fey, A. and Charlot, P., “VLBA Observations of Radio Reference Frame Sources. II. Astrometric Suitability Based on Observed Structure”, 1997, ApJS, 111, 95.